Environmental controls on ecosystem-scale cold season methane and carbon dioxide fluxes in an Arctic tundra ecosystem.

Dean Howard[a,b], Yannick Agnan[c], Detlev Helmig[a], Yu Yang[d], and Daniel Obrist[b]

[a]Institute of Arctic and Alpine Research, University of Colorado Boulder, Boulder, CO, USA
[b]Department of Environmental, Earth and Atmospheric Sciences, University of Massachusetts Lowell, Lowell, MA, USA
[c]Earth and Life Institute, Université Catholique de Louvain, Louvain-la-Neuve, Belgium
[d]Department of Civil and Environmental Engineering, University of Nevada, Reno, NV, USA

Correspondence: Daniel Obrist (Daniel_Obrist@uml.edu)

Abstract. Understanding the processes that influence and control carbon cycling in Arctic tundra ecosystems is essential for making accurate predictions about what role these ecosystems will play in potential future climate change scenarios. Particularly, air–surface fluxes of methane and carbon dioxide are of interest as recent observations suggest that the vast stores of soil carbon found in the Arctic tundra are becoming more available to release to the atmosphere in the form of these greenhouse gases. Further, harsh wintertime conditions and complex logistics have limited the number of year-round and cold season studies and hence too our understanding of carbon cycle processes during these periods. We present here a two-year micrometeorological data set of methane and carbon dioxide fluxes that provides near-continuous data throughout the active summer and cold winter seasons. Net emission of methane and carbon dioxide in one of the study years totalled 3.7 and 89 g C m^{-2} a^{-1} respectively, with cold season methane emission representing 54% of the annual total. In the other year, net emission totals of methane and carbon dioxide were 4.9 and 485 g C m^{-2} a^{-1} respectively, with cold season methane emission here representing 82% of the annual total – a larger proportion than has been previously reported in the Arctic tundra. Regression tree analysis suggests that, due to relatively warmer air temperatures and deeper snow depths, deeper soil horizons – where most microbial methanogenic activity takes place – remained warm enough to maintain efficient methane production whilst surface soil temperatures were simultaneously cold enough to limit microbial methanotrophic activity. These results provide valuable insight into how a changing Arctic climate may impact methane emission, and highlight a need to focus on soil temperatures throughout the entire active soil profile, rather than rely on air temperature as a proxy for modelling temperature–methane flux dynamics.

1 Introduction

Active-layer soils and permafrost soils in the Arctic permafrost region contain significant stores of terrestrial organic carbon. These ecosystems account for an estimated 1307 (1140–1476) Pg of organic carbon, with ∼1035 Pg found within soils between 0 and 3 m depth (Hugelius et al., 2014). Recently-observed increases in surface air temperature within these regions (Polyakov et al., 2002) have sparked interest in the biogeochemical cycling of this carbon store, as substrate metabolic activity — shown to be positively correlated to temperature — can break down organic compounds in the soil, releasing soil organic carbon to

the atmosphere in the form of carbon dioxide and methane (Lai, 2009). Furthermore, the "active layer" horizon, within which

25 most soil carbon decomposition takes place, has been observed in places to be expanding as the underlying permafrost thaws under the influence of a warming atmosphere, thus exposing larger quantities of organic carbon to decomposition (Schuur et al., 2009; Romanovsky et al., 2010; Schuur et al., 2015; Vonk and Gustafsson, 2013).

Production of methane in the carbon-rich soils of the Arctic tundra takes place as a result of microbial metabolic activity (Lai, 2009). The break-down of organic carbon to form methane is a complex process that requires contributions from various

30 taxa of microorganisms (Whalen, 2005). Methanogens form the last step in this process of producing methane from organic polymers (Conrad, 1999); whilst these methanogens encounter oxygen in the breaking down of acetate and carbon dioxide, they cannot survive in oxic environments (Whalen, 2005; Kamal and Varma, 2008; Lai, 2009). As such, methanogenesis in peatlands is an obligate anaerobic process that takes place largely within deeper, anoxic layers of the soil, generally below the water table level (Le Mer and Roger, 2001). Methane production at these depths creates concentration gradients that lead to

35 upward diffusion of methane through the soil to the surface (Preuss et al., 2013). Furthermore, methane can be transported to the surface via ebullition and through aerenchymatous tissues within some vascular plants (Joabsson et al., 1999; Lai, 2009).

In the upper soil layers, another subset of microorganisms known as methanotrophs consume a portion of this produced methane in the presence of oxygen, eventually oxidising it to carbon dioxide (Lai, 2009). These methanotrophs are largely exposed to methane diffusing through the soil pore space, as ebullition is too quick to allow exposure to methanotrophs (Boone,

40 2000) and plant vascular transport shields methane from methanotrophic activity (Schimel, 1995; King et al., 1998; Verville et al., 1998). The rate of methane consumption is usually highest immediately above the water table level, where high concentrations of methane formed from the underlying methanogens meet with sufficient oxygen levels from the overlying atmosphere (Dedysh et al., 2002). Rates of both methanogenesis and methanotrophy are highly dependent on temperature, with optimal metabolic rates (as determined in the laboratory) occurring at temperatures of around 25 °C (Dunfield et al., 1993). Of the two

45 competing processes, methanogenesis has shown to be more temperature-dependent with higher reported rate changes per unit warming (e.g. per 10 °C (Q_{10}): 5.3–16) compared to methanotrophy (Q_{10}: 1.4–2.1) (Dunfield et al., 1993).

Estimating the methane exchange budget in Arctic tundra ecosystems and how it relates to temperature are challenging objectives, currently subject to considerable uncertainties. Ambient observations in northern Alaska over 29 years showed no clear increase in ambient atmospheric methane concentration enhancements during this period, despite noticeably warmer air

50 temperatures (Sweeney et al., 2016). Direct observations of methane exchange, however, during the Carbon in Permafrost Experimental Heating Research (CiPEHR) project, showed significant increases in methane emission under warming soil conditions (Natali et al., 2015). Multi-year carbon exchange data sets are rare, and challenging winter conditions at Arctic sites has led to many studies focussing largely on summer and early autumn periods (Euskirchen et al., 2012). The first year-round micrometeorological methane exchange measurements reported showed that cold season methane emission dominated

55 the annual exchange budget, suggesting a predominant role of cold-season processes (Zona et al., 2016). At five Alaskan sites, substantial methane emission occurred throughout the cold season, and although emission rates were lower than those measured during the warmer summer period, prolonged wintertime activity amounted to 50% ± 9% (mean ± 95% confidence

interval) of annual emission. The authors suggest that this cold season emission may become more important under forecasted climate conditions that include higher air temperatures and deeper snowpacks (Hay and McCabe, 2010; Zona et al., 2016).

60   We present here a two-year micrometeorological methane and carbon dioxide exchange data set, undertaken over an acidic tussock tundra site near the Toolik Field Station, Alaska, USA, on the north slope of the Brooks Range. Complimentary to air–surface exchange measurements, we report soil pore space methane, carbon dioxide and oxygen concentrations and soil water content in the upper 40 cm, as well as soil temperature profiles at and near the site to a depth of 150 cm. All measurement systems were deployed year-round, providing near-continuous data coverage throughout both the summer growing seasons

65   and the cold winter seasons in both years. The goal of this study was to investigate environmental controls that significantly impact the magnitude and direction of methane fluxes in this environment – particularly over the colder winter months – as environmental control–methane flux relationships during these periods are relatively poorly understood. These results add to our growing understanding of carbon exchange dynamics in the Arctic tundra soils, as well as provide insights into how these dynamics may evolve under forecasted changing conditions in this environment

70 2   Methods

2.1   Site description

This study was performed over two full years from October 2014 to September 2016 at Toolik Field Station (Alaska, USA) located on the north slope of the Brooks Range (68° 38' N, 149° 36' W, 720 m a.s.l.). The study site, approximately 180 km south of the Arctic Ocean, overlies Cretaceous shale, claystone, siltstone, and sandstone, with soils that are characterised

75   as cryosols. Vegetation within the measurement footprint (see Fig. S1) is dominated by an acidic tussock tundra vegetation: scrubby plants (e.g. *Cassiope tetragona* (L.) D.Don, *Arctostaphylos alpinus* (L.) Spreng.), shrubs (e.g. *Betula nana* L., *Salix pulchra* Cham.), tussock grasses (*Carex*), mosses and lichens (Shaver and Chapin III, 1991). Vegetation in other areas of the measurement footprint were characterised as wet graminoid tundra (sedge and moss tundra). Both mineral and organic soil profiles were closely present together with different horizon depths. Soil organic carbon content, based on eight soil sampling

80   pits to a depth of 90 cm around the flux tower, was highly variable, with A-horizon organic carbon concentrations averaging 10.3% (range of 7 to 14%) and B-horizon organic carbon concentrations averaging 2.4% (range of 1 to 4%) (Olson et al., 2018). Estimates of soil organic carbon density in the flux footprint range from 5 to 25 g C m^{-2} (Fig. S2).

2.2   Instrumentation

An aerodynamic gradient approach was utilised for observing air–surface methane and carbon dioxide fluxes. Turbulent char-

85   acteristics were measured using a Metek USA-1 sonic anemometer (Metek GmbH, Elmshorn, Germany), positioned 2.36 m above the tundra soil. Atmospheric sampling of trace gas concentrations was performed at heights $z_1 = 0.61$ m and $z_2 = 3.63$ m. Perfluoroalkoxy Teflon tubing from both the atmosphere and soil inlets were directed in a heated conduit to an onsite field laboratory, and a solenoid valve system allowed sequential sampling at both heights with switching interval of 10 minutes

(Obrist et al., 2017). Methane and carbon dioxide concentrations were quantified using a Los Gatos 915-0011 ultra-portable
greenhouse gas analyser (Los Gatos Research, Mountain View, CA, USA), factory-calibrated prior to installation and oper-
ating at 1 Hz. The analyser was zeroed using methane- and carbon dioxide-free zero air approximately every 6 weeks. Line
intercomparison tests were also performed with the same frequency by moving both inlets to the same height and sampling for
between 12 and 24 hours (average 17 hours). Concentration differences between the sample lines during the intercomparisons
were <0.001 μmol mol^{-1} for methane and <0.1 μmol mol^{-1} for carbon dioxide. Although the emphasis here is on methane
flux magnitudes and dynamics, carbon dioxide fluxes are discussed at length in order to understand corresponding respiration
processes that help us constrain the influence of microbial activity on observed methane fluxes.

Two soil profiles were installed between 15 and 20 m to the north of the flux tower (herein "Flux Tower" profiles), with
temperature and volumetric water content (VWC) measured at depths of 10, 20 and 40 cm. Temperatures were measured using
soil temperature probes (Model 107, Campbell Scientific Inc., Logan, UT, USA) and VWC was measured at the same depths
using time-domain reflectometry (Model CS615-L Soil Volumetric Water Reflectometers, Campbell Scientific Inc., Logan,
UT, USA). Further from the flux tower (430 m to the north-east), Toolik Field Station operates two profiles of soil temperature
(thermocouple) measurements to a depth of 150 cm (0, 5, 10, 20, 50, 100 and 150 cm). Despite the increased distance, these
profiles were included in the current analysis as they provide a longer time series (measurements have been taken continuously
since 1988) and information at deeper depths than the Flux Tower profiles. A snow tower (Seok et al., 2009; Faïn et al., 2013)
was installed prior to the first snowfall and recorded temperatures at 0, 10, 20, 30, 40 and 110 cm above the soil surface, thus
measuring temperatures within the snowpack as it developed above each measurement height. The average snowpack depth
over the site was measured daily using a camera set to automatically record images of reference snow stakes (Agnan et al.,
2018). These depth measurements began in November 2014, and so the first snowfalls in that year were not recorded.

2.3 Calculations

Fluxes of methane and carbon dioxide were calculated using the aerodynamic gradient approach described by Edwards et al.
(2005):

$$F = \frac{-ku^*(C_2 - C_1)}{\ln((z_2 - d)/(z_1 - d)) - \Psi_2 + \Psi_1},$$ (1)

where F represents the flux of either methane or carbon dioxide, k the von Kármán constant, u^* the friction velocity, C_i
the concentration of atmospheric trace gas species in question at height $i = [1, 2]$, z_i the sampling height, d the displacement
height and Ψ_i the stability-dependent integrated similarity functions for heat, as given by Businger et al. (1971). Herein we
follow the convention of positive flux values representing emission, whilst negative values represent deposition.

Atmospheric turbulent characteristics (friction velocity and Obukhov stability) were calculated using the flux processing
software EddyPro v.6.2.0 (Li-COR, Lincoln, NE, USA) using 30-minute averaging periods. Rotation of sonic data into mean
wind vectors was accomplished using the double rotation technique and quality control tests for steady state and developed
turbulent conditions were implemented according to Foken et al. (2004). Apparent sonic anemometer sampling height was

altered according to daily observed snow depth in increments of 5 cm, as were gradient intake sampling heights. As a single instrument was used for trace gas sampling at both intake heights, leading to a loss of temporal coverage within each 30-minute period (Woodruff, 1986), gaps in the concentration time series were estimated for each averaging period using a 4th order polynomial fit to the observed concentration time series. Average concentrations at each height were then calculated from

125 a truncated mean (10th–90th percentile) in order to reduce effects of outliers (Fig. S3).

Two-dimensional footprint analyses were undertaken for each 30-minute period using the method of Kljun et al. (2015) and fluxes for which the footprint intensity over the adjacent Toolik Lake was shown to be >20% of the total were removed from analysis. Analysis of energy balance closure showed that calculated turbulent and soil heat fluxes for snow-free periods, excluding fetches in the direction of Toolik Lake, accounted for approximately 88% of net radiative fluxes (linear least

130 squares, $p <0.001$). Gaps in both methane and carbon dioxide fluxes, resulting from quality control and instrument downtime/maintenance, were filled using the R package REddyProc (Wutzler et al., 2018). The efficacy of this gap filling was tested against a randomly-selected validation set of size equal to 10% of available flux values (Fig. S4). Ecosystem respiration was approximated using gap-filled carbon dioxide fluxes, filtered to exclude times when incoming photosynthetically active radiation (PAR) was above 5 μmol m^{-2} s^{-1} (Natali et al., 2015). Periods during which no data fitting this criteria are available (i.e.

135 polar day) were not gap-filled, resulting in incomplete temporal coverage for ecosystem respiration.

3 Results and Discussion

3.1 Site climatology

Air temperatures, as observed at Toolik Field Station, showed similar patterns and magnitudes between 2014–15 and 2015–16, ranging between -40 °C and 0 °C during the winter months and -5 °C and 20 °C during the warmest summer months (Fig.

140 S5). Air temperatures in these years also remained within the range of those observed during the preceding 26 years during all months of the year. Soil temperatures at 20 cm depth were within the expected climatological range during the summer months, however throughout the colder months (between mid-November and late April), temperatures during 2014–15 and 2015–16 were among the warmest observed since 1988. Likewise, at 100 cm depth, wintertime soil temperatures during 2014–15 and 2015–16 were among the warmest seen in the Toolik Field Station record. Minimum cold season soil temperatures at

145 these depths for 2014–15 and 2015–16 were the second- and third-highest on record, respectively (Fig. S6). To investigate the climatological influence of atmospheric forcing on soil cooling, Fig. S6 also shows that 2014–15 had the shortest cold season (defined in this instance as the period during which the 28-day running mean of 5 m air temperature remains below 0 °C) and the third-smallest freezing degree day (FDD) value on record. Whilst 2015–16 had an average-length cold season (20th shortest on record), it had the fourth-smallest FDD value since 1988.

150 Though snow depth has not been measured at Toolik Field Station across the same period of time, observations at the snow tower provide some additional insights into why soils were warmer during the winter of 2014–15 compared to 2015–16 (Fig. S7). Snow depth was significantly (Student's t-test, $p <0.001$) larger in 2014–15 (mean 32 cm) than in 2015–16 (mean 22 cm). Deeper snowpacks are able to provide an increased thermoinsulation effect from cold air temperatures, particularly in the

early cold season (Maksimova et al., 1977; Sokratov and Barry, 2002), thus leading to warmer and less variable surface soil
155 temperatures. This effect can be seen in the temperature pulses shown in the snow tower thermocouple data (Fig. S7) and their
effect on the underlying soil, where the minimum subnivean surface temperature in 2014–15 (-12 °C) was 5 °C warmer than
that observed in 2015–16 (-17 °C).

Arctic tundra ecosystems are highly heterogeneous within the scale of micrometeorological flux footprints (typically 10s
to 100s metres Kljun et al., 2015; Fox et al., 2008), and during the winter, the combined effects of wind and topography
160 lead to even greater spatial heterogeneity in snow depths and snow physical properties (Agnan et al., 2018). Sub-surface soil
temperatures, which are further influenced by air temperature and downwelling radiation; overlying vegetation and snow; and
soil properties and moisture, are likely highly spatially variable within the footprint as well. As a result, the limited number
of soil temperature profiles within the flux measurement footprint may not be fully representative of the average temperature
within the flux footprint. The four soil temperature profiles we have available are separated both in space and in the soil
165 properties in which they were installed. Fig. S8 shows the time series for each of these profile measurements at two common
depths (10 and 20 cm). This time series shows that, whilst the absolute range of temperatures between measurements can be
pronounced, the correlation between these soil temperature measurements is reasonable enough throughout most of the study
period (mean $R^2 = 0.64$) to warrant use of Toolik Field Station data for further investigation of temporal trends. The decision
to use Toolik Field Station data was driven primarily by the deeper profiles measured here, as this information is vital to the
170 primary outcomes of this study (see Section 3.4).

3.2 Annual and seasonal flux patterns

Half-hourly methane and carbon dioxide fluxes are shown in Figure 1, along with total cumulative values over the ~two-year
(727-day) study. Overall, based on combined raw and gap-filled data, the mean half-hourly methane flux showed an emission of
0.5 ± 0.5 mg C m^{-2} h^{-1} (herein, uncertainty is expressed as one standard deviation of the measured values). The distribution
175 of methane fluxes (Fig. S9) showed a positive skew, as well a secondary peak in values close to zero. Cumulative diel sums
gave a mean net daily flux of 11 ± 8 mg C m^{-2} d^{-1}. Over the study period as a whole the site acted as a net source of methane,
with a cumulative methane emission of 8.6 g C m^{-2} (4.9 g C m^{-2} and 3.7 g C m^{-2} in the first and second years, respectively).
The overall mean carbon dioxide flux across the two years of measurements was 0.0 ± 0.2 g C m^{-2} h^{-1} (mean net daily flux of
1 ± 3 g C m^{-2} d^{-1}), with the site acting as a net source of carbon dioxide during both years of measurements. The distribution
180 of carbon dioxide fluxes across the study (Fig. S9) did not show skewness as seen in the methane flux distribution, though it did
show a higher level of kurtosis. During the 24-month measurement period, the site emitted a net carbon dioxide flux equivalent
to 583 g C m^{-2} (485 g C m^{-2} and 89 g C m^{-2} in the first and second years).

Seasonality can be defined in a number of different ways depending on the processes of interest (Mastepanov et al., 2013);
initially, we followed similar definitions as those described by Zona et al. (2016) who investigated changes in methane fluxes
185 based on surface (10 cm) soil temperatures. Periods where surface soil temperatures were above 0 °C were defined as "active"
seasons (yellow shading in Fig. 1) and those where soil temperatures were below 0 °C were defined as "frozen" seasons (blue
shading in Fig. 1). Zero curtain periods, where surface soil temperature remains close to 0 °C (± 0.5 °C) for prolonged

time periods due to latent heat released or absorbed from soil water, were separated into "freezing" or "thawing" seasons.
Freezing seasons (turquoise shading, Fig. 1) occurred prior to the frozen season, whilst thawing seasons (green shading, Fig.
190 1) occurred after the frozen season and prior to the active season. Combined freezing–frozen–thawing periods were defined as
"cold season". The period from the onset of the freezing season in 2014 until the end of the active season in 2015 has herein
been defined as "Year 1", whilst the same seasons from 2015 until 2016 have been defined as "Year 2". Tables 1 and 2 give
summary methane and carbon dioxide flux data, respectively, for these seasons and years so defined.

Table 1 shows marked differences in the magnitude and seasonality of methane fluxes between the two years. Cumulative
195 methane emission in Year 1 was 1.3-fold that of Year 2, across a slightly shorter period (347 days compared to 380 days). All
seasons showed net methane emission across the study period, with statistically significant differences (Student's two sample
t-test, $p < 0.05$) in the net daily flux between Year 1 and Year 2 for all seasons. The largest seasonal differences in net daily
methane fluxes between years were for the active and frozen seasons (6 and 10 mg C m^{-2} d^{-1}, respectively). For Year 2, the
active season showed significantly higher methane emission compared to Year 1, releasing 1.7 g C m^{-2} (15 mg C m^{-2} d^{-1}),
200 or 46% of the annual total, compared to 0.9 g C m^{-2} (9 mg C m^{-2} d^{-1}), or 18% of the annual total for Year 1. Conversely,
the frozen season showed higher emission in Year 1, releasing 2.5 g C m^{-2} (16 mg C m^{-2} d^{-1}), or 51% of the annual total,
compared to 1.1 g C m^{-2} (6 mg C m^{-2} d^{-1}), or 30% of the annual total in Year 2. Year 1 also showed higher methane emission
in the freezing and thawing seasons, though these represented similar percentages of the annual total across both years ($\sim$25%
of annual total for freezing and 3–4% of annual total for thawing). Zona et al. (2016) reported average cold season methane
205 emission from five Alaskan Arctic sites of 1.7 $\pm$ 0.2 g C m^{-2}, accounting for between 37 and 64% of the total annual methane
budget at these sites. The authors note that these contributions are higher than those estimated from previous models and
periodic chamber observations. In our study, observations in Year 2, where 50% of annual methane emission occurred in the
cold season, are within the ranges reported by Zona et al.. However, cold-season methane emission during Year 1 accounted
for 82% of annual net emission, indicating that cold-season methane emission can strongly dominate annual flux magnitudes,
210 to a larger extent than recent evidence suggests.

Figure 1a shows the detailed temporal patterns that help explain differences in seasonal net emission between the two years.
For Year 1, the 28-day moving average (herein MA28) methane flux (red line in Fig. 1a) was initially relatively high and positive
at the onset of the freezing season ($\sim$1 mg C m^{-2} h^{-1}), and remained at a similarly high level during the Year 1 freezing season
and most of the frozen season. In early March 2015, the MA28 methane flux began to steadily decline during the late frozen
215 season, thawing season, and mid-way into the active season, reaching a minimum emission of $\sim$0.1 mg C m^{-2} h^{-1} in August
2015 before increasing again to $\sim$0.7 mg C m^{-2} h^{-1} at the onset of the Year 2 freezing season in September 2015. In contrast,
in the Year 2 freezing season, MA28 methane flux began to decline in October 2015, and continued a consistent and relatively
constant decline throughout the winter until it approached $\sim$0.2 mg C m^{-2} h^{-1} in February 2016. It was not until the thawing
season in June 2016 that the MA28 methane flux again began to increase in magnitude (net positive), reaching a peak of
220 $\sim$0.9 g C m^{-2} h^{-1} about mid-way through the Year 2 active season.

Carbon dioxide fluxes (Table 2) showed significant net emission throughout the entire cold season in Year 1 (471 g C m^{-2}
or 1.9 g C m^{-2} d^{-1}), followed by minor net emission in the subsequent active season (14 g C m^{-2} or 0.1 g C m^{-2} d^{-1}). Year

2 freezing and frozen seasons showed lower carbon dioxide emission than Year 1, and the thawing season showed net carbon dioxide deposition, resulting in a combined cold season emission of 294 g C m^{-2} or 1.1 g C m^{-2} d^{-1} (38% lower than Year 1). Net active season carbon dioxide fluxes in Year 2 showed significant deposition, at -211 g C m^{-2} or -1.9 g C m^{-2} d^{-1}.

225 Annual and multi-season micrometeorological flux studies are rare for the Alaskan Arctic (Commane et al., 2017); however, the net annual carbon dioxide flux for Year 2 is within the range of values reported for wet sedge tundra (2 to 147 g C m^{-2} a^{-1} Euskirchen et al., 2012, 2017), and larger than for heath tundra (21 to 61 g C m^{-2} a^{-1} Euskirchen et al., 2012, 2017) or tussock tundra (13 to 15 g C m^{-2} a^{-1} Euskirchen et al., 2012; Oechel et al., 2014). The net annual carbon dioxide flux was significantly above the range previously reported for wet sedge tundra. Arctic tundra ecosystems are highly heterogeneous

230 both physically and biogeochemically (Fox et al., 2008) and the area examined here is no exception. Seasonal two-dimensional footprint analyses (Fig. S10) showed a prdeominantly southerly footprint during all seasons, where fens and moist tundra are more abundant (Fig. S1). Importantly, the homogeneity in all seasonal footprints shown in Fig. S10 excludes the possibility that observed differences in seasonal flux magnitudes (i.e. higher cold season contributions in Year 1 relative to Year 2) are due to flux footprint differences over heterogeneous surfaces.

235 Figure 1b shows the detailed temporal patterns of seasonal net carbon dioxide emission for the two years. Active season net carbon dioxide sinks in both years are consistent with long-term eddy covariance observations that show summertime sink trends in the Alaskan Arctic (Oechel et al., 2008). These active season carbon dioxide sinks also are consistent with large-scale aircraft observations over the Alaskan North Shore tundra (Commane et al., 2017) that show a switch to carbon dioxide

240 uptake during June–August, peaking at approximately -0.3 g C m^{-2} h^{-1}. Cold season MA28 carbon dioxide fluxes are almost consistently positive, only switching to net uptake in the late thawing season of Year 1. A major distinction between the two years of measurements is the duration of relatively high emission – also noted by Commane et al. – that begins in the late active season and extends into the freezing season. As shown in Figure 1b, while MA28 carbon dioxide emission decreased relatively early in Year 2, dropping below 0.1 g C m^{-2} h^{-1} in October 2016, in Year 1 this decline occurred at a slower rate,

245 remaining relatively high and not reaching the same low value until January 2015. Importantly, in both years, MA28 carbon dioxide fluxes do not completely cease during the cold season and always maintain a small emission throughout winter (up to 0.1 g C m^{-2} h^{-1}).

In summary, the two years showed substantial temporal differences in methane fluxes, with Year 1 showing higher methane emission throughout most of the cold season (100% greater), contributing a high fraction (82%) of annual net methane emis-

250 sion. This is in contrast to Year 2, which experienced a continued decline in methane emission that began early in the freezing season, resulting in a relatively low contribution (54%) to the annual total. Annual carbon dioxide flux magnitudes were most similar to other wet sedge tundra measurements; show strong seasonal trends with relatively high respiration in the freezing season and prolonged but low carbon dioxide emission in the frozen season; and carbon dioxide uptake during the thawing and/or active season, largely in agreement with carbon dioxide flux patterns reported for northern tundra ecosystems before.

255 Inter-annual comparison, however, showed cold-season carbon dioxide fluxes that were 38% higher in Year 1, also largely driven by slower and later declines in carbon dioxide emission fluxes during the freezing and frozen periods.

3.3 Soil temperature relationships

Continuous cold season methane flux data at the ecosystem level are rare for Arctic tundra ecosystems. Given the strong dominance of cold-season fluxes for annual flux magnitudes (54% to 82% in our study), the pronounced differences in cold season

260 methane flux dynamics between the two years merit particular attention. Methane flux dynamics are controlled largely by soil methanogenic and methanotrophic activity (Lai, 2009), and previous research has suggested that, in frozen soils (where water table dynamics become less important), soil temperature has the strongest control on microbial activities that drive methane production and consumption (Le Mer and Roger, 2001). In order to maintain comparability with similar year-round methane flux observations in the Alaskan Arctic (Zona et al., 2016), our initial investigations into relationships between ecosystem-level

265 methane fluxes and underlying soil temperatures began with soil temperatures measured at 10 cm depth (hereafter surface soil temperature). This is shown in the upper panels of Figure 2, where MA28 methane fluxes are plotted against MA28 surface soil temperatures, as measured at the Toolik Field Station. Horizontal lines show the spread of all available surface soil measurements (i.e. both at Toolik Field Station and closer to the flux tower).

Based on these upper panels in Figure 2, it is evident that methane fluxes showed very different relationships with surface

270 soil temperature in Year 1 compared to Year 2. For Year 2 (Fig. 2b), we observed a pattern similar to that reported by Zona et al. (2016), whereby MA28 methane fluxes began to decrease mid-way through the freezing season (point F, October 2015). As surface soil temperatures continued to decrease during the frozen season (F–G), MA28 methane fluxes continued to decline, reaching a minimum during the frozen season in March 2016 (point G). MA28 methane fluxes remained low (between 0.1 and 0.2 mg C m^{-2} h^{-1}) during the remaining frozen season, as MA28 surface soil temperatures increased from its minimum

275 of -5.1 °C to 0 °C (G–H). As surface soil temperatures continued to warm above 0 °C during and beyond the late thawing season, methane emission increased significantly into the active season (H–I), peaking in August 2016 (point J). The relationships observed in Year 2 provide evidence that surface soil temperature is correlated with cold season methane fluxes, yet with substantial variability and a strong hysteresis between freezing and thawing periods. Zona et al. (2016) suggested that temperature-dependent decreases in the near-surface methane oxidative capacity were largely responsible for the slow atten-

280 uation of methane fluxes in the early frozen period (here F–G), noting that sites with the largest and warmest active layers displayed the slowest decrease in methane fluxes. Soil pore gas concentration measured in our study show that oxygen levels within the upper 40 cm were sufficient (>17%) to ensure methane oxidation in this zone across the entire study period and hence that the top 40 cm soils were continuously oxic (data not shown). We also note that soil pore gas measurements took place in an elevated, drier tussock region and that the thickness of the upper oxidative region is expected to be smaller in lower

285 depression areas and more water-saturated wet sedge regions (Gebauer et al., 1996). Due to the dominance of methanotrophic microbial communities in the upper oxic region, surface soil temperatures are likely an underlying reason, and hence a good predictor, for observed declines in freezing season methane emission. However, the strong Year 2 active season increase in methane emission is unlikely causally related to surface soil temperatures, as methanogenic microbial communities are less abundant in the upper 40 cm of soils. Instead, as suggested by Zona et al., increases in methane emission as surface soils warm

290   above 0 °C (points H–I in Fig. 2b) are likely coincident with enhanced methanogenic activity as temperature pulses reach deeper anoxic soil layers (see Section 3.4).

     In contrast to Year 2, Year 1 MA28 methane fluxes showed almost completely reversed relationships with surface soil temperatures (Fig. 2a). MA28 methane fluxes remained high (mean 0.8 mg C m^{-2} h^{-1}) throughout the freezing and early frozen seasons in spite of temperatures decreasing below freezing (A–B), with values among the largest observed across

295   the entire study period. Methane fluxes only began to decrease after March 2015 (point B) as MA28 surface temperature approached its minimum value of that season (-2.6 °C). Thereafter, methane fluxes continued to decline, even as surface temperature began to increase again in the remaining frozen and thawing seasons, as well as partway into the active season (B–C). The Year 1 minimum MA28 methane flux of 0.1 mg C m^{-2} h^{-1} occurred during the active season (point E, August 2015). During the active season, relationships between surface temperature and MA28 methane fluxes were highly variable, showing

300   both positive and negative correlations. These data from Year 1 that show in parts inverse relationships between methane flux and surface soil temperature (relative to Year 2 and Zona et al. (2016)) suggest that, under certain conditions, surface soil temperature alone cannot always reliably predict seasonal methane flux patterns. In fact, that some of the highest methane emission observed during the period of coldest surface soil temperature in the Year 1 cold season is in direct contrast to the strong temperature-dependence of microbial activity reported by Zona et al. (2016).

305   Figure 2c,d similarly display relationships of MA28 net ecosystem respiration with MA28 surface soil temperature, whereby ecosystem respiration is approximated as carbon dioxide fluxes during periods when incoming PAR is less than 5 μmol m^{-2} s^{-1}. Note that this approach only provides an upper boundary for heterotrophic microbial activity as autotrophic respiration by plants also contributes to observed carbon dioxide fluxes (Hicks Pries et al., 2015). These panels show that, in both years, MA28 respiration fluxes decreased rapidly during the onset of both freezing seasons as soil surface temperature cooled, from 0.3 to

310   0.0 g C m^{-2} h^{-1} (Year 1) and 0.2 to 0.0 g C m^{-2} h^{-1} (Year 2). As surface soils cooled further during the frozen seasons, respiration fluxes remained low, with Year 2 frozen season MA28 respiration fluxes decreasing from 0.04 to 0.01 g C m^{-2} h^{-1}, whilst in Year 1 these values were more variable, declining from 0.1 g C m^{-2} h^{-1} to near-zero before increasing again to 0.05 g C m^{-2} h^{-1}. Respiration fluxes increased in both years prior to and during the thawing periods as surface soils warmed. It is noteworthy that the beginning of these increases coincided with turning points in the MA28 methane flux-surface tem-

315   perature relationship (points B and G). In the active season, as discussed previously, Year 2 showed higher net carbon dioxide emission than Year 1. Similarly, since surface soil temperatures were much warmer in the Year 1 cold season, heterotrophic respiration in this upper oxic soil region remained high relative to Year 2 leading to higher cold season cumulative carbon dioxide losses (Table 2). The strong relationships between cold season ecosystem respiration fluxes and surface soil temperature, and the relative similarity between the two years, is consistent with patterns reported in previous research (Lüers et al., 2014;

320   Euskirchen et al., 2012; Björkman et al., 2010), and largely explain differences in the temporal trends of ecosystem respiration flux between the two years. This result suggests that changing heterotrophic microbial respiration in the upper soil region is not a suitable explanation for the differences in methane flux–surface soil temperature relationships observed between Years 1 and 2.

3.4 Regression tree approach to seasonal methane flux dynamics

325 As discussed above, methane fluxes are largely dependent on microbial processes that compete in outcome (i.e. methanogenesis vs. methanotrophy), yet show similar environmental dependencies (Le Mer and Roger, 2001). Previous soil methane studies have shown a range of controlling factors on microbial activity related to both methanotrophic and methanogenic activities, including temperature, water table depth, oxygen availability and Eh, soil organic matter content, soil pH, soil texture and soil mineralogy, though soil temperature and water table depth are often identified as the major of these controlling factors (Le

330 Mer and Roger, 2001; Yvon-Durocher et al., 2014; Gulledge et al., 1997). We employed a regression tree approach (Sachs et al., 2008) to explore non-linear relationships between observed methane fluxes and variables identified in the literature as influential to methanotrophic/methanogenic activity. Of the known variables, soil organic carbon content, pH, texture and mineralogy cannot explain changes in fluxes over short time periods and hence were not included. Additionally, pore-space oxygen concentrations were not included in the analysis since it was measured only in the upper 40 cm and remained oxic

335 throughout the entire study period. For the regression tree, we hence used soil temperature data from the surface to 150 cm depth, as well as surface VWC. Daily values were chosen in order to reduce the influence of diel variability, with net daily sums (in the case of methane fluxes) and mean daily values (for temperature and water content) as inputs into the model. The outcome of this analysis is shown in Fig. 3a, along with the time series of net daily methane fluxes used to build the model (Fig. 3b). Horizontal lines and coloured shading in Fig. 3b show mean ± one standard deviation of the input methane flux data,

340 as grouped by the predictive model. The predictive capability of this model, tested against a randomly-selected validation set representing 10% of the available input data, shows an R^2 value of 0.69 ($p <$ 0.001).

The two variables that most effectively cluster methane flux values within the hyper-dimensional data space are soil temperatures measured at 100 cm and at 10 cm depths. Critically, these two temperature variables separate, and likely explain, substantial methane flux differences observed during the frozen seasons between Year 1 and Year 2. Specifically, the frozen

345 season in Year 2 was largely represented by regression tree outcomes when temperatures at 100 cm soil depth were below -2.4 °C, marked in Fig. 3b in blue and red. This is the only season during the study period when 100 cm soil temperature fell below this threshold (see also Fig. 4). Measurements throughout the active layer by Gebauer et al. (1996) at nearby Imnavait Creek suggest that it is highly likely that soils at these depths are anoxic and thus methanogenesis is the dominant relevant microbial process taking place here. In contrast to Year 2, the Year 1 frozen season was largely separated from the remainder of

350 the study period (with 100 cm soil temperatures above -2.4 °C) when 10 cm temperatures were simultaneously below -0.6 °C (purple and green shading). During this season, methane emission values were amongst the highest observed throughout the entire study period. As discussed previously, our own soil pore gas measurements show that these surface soils are oxic and thus methanotrophy is here likely the dominant relevant microbial process. It must be noted that these temperature thresholds do not represent mechanistic limits but instead the most effective clustering of observed data, based on the chosen environmen-

355 tal parameters. Even so, the reasonably good predictive capability of this model provides strong evidence that a critical reason for strong flux differences between frozen season methane fluxes was differences in deep soil temperature between the two years. More precisely, these first two results from the regression tree analysis show a threshold temperature value at a depth

of approximately 100 cm that is linked to low methane emission in Year 2, and an additional threshold temperature value at a depth of approximately 10 cm that is linked with high frozen season emission in Year 1.

360 A decrease in methanogenesis below a temperature threshold around -2.4 °C as suggested by the model is in reasonable agreement with several experimental laboratory studies. Incubation studies investigating the temperature dependency of methanogenesis in Arctic soils have shown that it can take place at sub-zero temperatures, though at greatly reduced rates. Rivkina et al. (2004) reported substantial methane production at temperatures of -1.8 °C in Siberian permafrost soils, as well as methane production in these soils at temperatures as low as -16.5 °C, though at a rate 100 times lower than at -1.8 °C.

365 Similarly, Panikov and Dedysh (2000) observed minor methane emission from Siberian peat bog soils at -20 °C that increased by an order of magnitude after thawing. Chowdhury et al. (2015), using soils from Barrow, Alaska, showed evidence of substantial methanogenesis in organic and mineral active layer soils kept at 4 and 8 °C, yet this was not observed in permafrost soils or in active layer soils kept at -2 °C. Similarly, for methanotrophic activity, temperature dependencies have also been observed, again with lower microbial activity reported at lower soil temperatures. Jørgensen et al. (2015) reported an expo-

370 nential relationship between temperature and methane uptake in unsaturated Arctic tundra soils. At 18 °C they observed a deposition flux of 192 μg C m^{-2} h^{-1} – this decreased to 24 μg C m^{-2} h^{-1} in soils kept at -4 °C. Richter (2019) also observed a temperature-related decrease in methane oxidation in A- and B-horizon soils sampled near Toolik Lake, to below detection levels at temperatures below -2 °C. Based on this evidence and our regression tree analysis, we suggest that the separation of methane fluxes in the Year 2 frozen season (the period with the lowest methane fluxes across the entire study period) is linked

375 to an inhibition of methane production due to low soil temperatures in deep, anoxic soil horizons. Further, we suggest that the separation of methane fluxes in the Year 1 frozen season (the period with some of the highest methane fluxes across the entire study period) is linked to an inhibition of methane oxidation due to low soil temperatures in oxic, surface soil horizons.

The full time series of interpolated soil temperature profile measurements at Toolik Field Station is shown in Fig. 4, along with the -2.4 °C isotherm identified in the first grouping of the regression tree analysis. These profile data show clearly that

380 the deeper soil horizons never reached the cold temperatures in the Year 1 frozen season that they did in the Year 2 frozen season – in fact, the -2.4 °C isotherm did not move below 70 cm depth in Year 1. The MA28 methane flux (black line, lettering corresponds in time to that given in Fig. 2) shows cold-season decreases that accompany cold temperature pulses into the deeper soil horizons. This is more readily seen in Year 2 (F–G) with the greater contrast in soil temperatures, though it is also noted that in Year 1 the onset of a decrease in methane emission (B–C) corresponds in time to a lowering of the -2.4 °C isotherm and

385 a still-perceptible cold temperature pulse to lower soil horizons. This highlights that the limits identified in the regression tree analysis (i.e. -2.4 ° at 100 cm depth) are not claimed to be mechanistic, yet they still provide valuable insight into competing methanogenic/methanotrophic processes within the soil profile. Frozen season differences in the MA28 respiration flux (green line) and, particularly, the ratio of methane flux to respiration (yellow line) further reiterate the disconnect between methane production and respiration that was highlighted in the discussion surrounding Fig. 2.

390 The shading in Fig. 3 shows that, whilst cold season methane fluxes could not be grouped together within the hyperdimensional data space for Years 1 and 2, freezing and thawing periods largely were. This suggests that the remaining seasonal methane flux dynamics can be related to the balance of continued methanogenesis at depth and methanotrophic activity near the

surface. Specifically, predicted methane fluxes outside the frozen seasons (orange, yellow, and brown shading) are separated according to temperatures at 150 cm and 20 cm, yet follow a similar pattern whereby colder temperatures at depth (suggesting

395 inhibited methanogenesis) and warmer surface temperatures (suggesting enhanced methanotrophy) jointly lead to smaller predicted methane fluxes (see also Fig. 4). One exception to these general patterns is during active seasons at times when surface VWC is greater than 0.65. During these periods the largest mean methane fluxes (as well as the largest methane flux variability) of any grouping were observed (pink shading). This observation is consistent with studies reporting increased methanogenic activity relative to methanotrophy under water-saturated soil conditions due to reduced oxygen diffusivity and highly reducing

400 conditions in otherwise oxic surface soils (Le Mer and Roger, 2001).

3.5 Implications for Arctic methane fluxes

Considerable debate exists over the potential future of methane fluxes in the Arctic tundra under future climates (Sweeney et al., 2016). Hydrologic modelling under IPCC forecasts by Hay and McCabe (2010) predicted warmer air temperatures with greater precipitation, leading to the suggestion that methane fluxes may increase as labile carbon becomes available due to permafrost

405 thaw. Warming experiments undertaken in the field in Alaska have also shown that warmer and wetter soils resulting from increased snow cover emit considerably more methane during the active period (Natali et al., 2015). Zona et al. (2016) stated that cold season fluxes made up to 64% of their reported annual methane emission, due to relatively low but consistent emission over a large portion of the year. We show here that cold season methane emission can account for an even greater percentage of the annual budget and that, under certain conditions, cold season emission fluxes are among the highest throughout the

410 year – as high as peak active season emission from saturated soils. Cold season methane fluxes are also subject to significant inter-annual variability. We further provided evidence that particularly high cold-season methane emission occurs when deep soil horizons are insulated and temperatures remain above the point where methanogenesis is efficient, while cold surface soil temperatures simultaneously minimise methanotrophic activity.

Modelled forecasting of Arctic methane fluxes is typically undertaken using air temperature data, due to its relative ease of

415 measurement and prediction, and the assumption that air temperature is closely linked to soil temperature (Riley et al., 2011; Koven et al., 2013; Zhu et al., 2014). An analysis of a 29-year record at Barrow, Alaska, however, showed no correlation between increasing air temperature and methane concentration anomaly (Sweeney et al., 2016), suggesting that air temperature is an inadequate variable for predicting methane fluxes. Air and soil temperature measurements at Toolik Field Station taken since 1988 (Fig. S6) show that, whilst Year 1 was the shortest winter (defined here once more as the period where MA28

420 air temperatures <0 °C) on record, both Year 1 and Year 2 were unusually warm and similarly ranked in regards to total FDDs (3rd and 4th warmest on record, respectively). Similarly, minimum cold season soil temperatures in the upper (20 cm) and deep (100 cm) horizons were unusually warm in both years, comparative to the long-term record (2nd and 3rd highest values, respectively). Given the relative similarity in the temperature anomaly of both years compared to the last 28, the large differences in cold season methane emission (2 times larger in Year 1 compared to Year 2) is unlikely related to a simple linear

425 relationship with increasing air, or even soil, temperatures.

Instead, we suggest the presence of a deep soil temperature *threshold* in anoxic horizons above which cold season methano-genesis – and hence net methane emission – remains high. Climatologically, there was little difference between Years 1 and 2 in terms of cold season FDDs, or minimum soil temperatures, relative to the previous 28 years. Yet, as suggested in the regression tree analysis and the temperature profiles in Fig. 4, any such temperature threshold was not crossed in the Year 1 cold season,

430 allowing methanogenesis to continue relatively unabated. Snow profile measurements (Fig. S7) show that, in addition to both winters experiencing relatively warm air temperatures, deeper snow in Year 1 likely insulated the underlying soil such that anoxic soil horizons cooled at a much slower rate. If, as has been predicted (e.g. Hay and McCabe, 2010), the Arctic continues to warm and precipitation increases, high methane emission winters will likely become more prevalent in the future, particu-larly also if enhanced summertime warming pulses penetrate deeper in the soil profile. Our observations highlight the need for

435 more sophisticated modelling of temperature regimes in the forecasting of methane emission. More importantly, we suggest that the increasing number of year-round ecosystem flux measurement sites operating in Arctic regions should monitor soil temperatures throughout the entire active soil region, rather than limit observations to the upper surface horizons. Temperature data throughout the entire active soil profile, preferably in conjunction with estimates of soil redox conditions, would help to further elucidate the competing microbial processes that drive methane fluxes at the surface.

440 ## 4 Conclusions

Year-round measurements of ecosystem-scale methane and carbon dioxide fluxes were undertaken at Toolik Field Station in the Alaskan Arctic over two years. Annual carbon dioxide exchange budgets suggest that these observations are representative of wet sedge tundra, with seasonal patterns that are characteristic of the Alaskan North Slope generally. Net methane and carbon dioxide fluxes in the Year 2 cold season (2.0 g C m^{-2} and 294 g C m^{-2} respectively, over 269 days) were similar in

445 magnitude to values reported in similar studies, and positive correlations between surface soil temperature and methane were observed as previously reported by Zona et al. (2016). Year 1 cold season net methane and carbon dioxide fluxes, however, were 100% and 38% higher, over a shorter cold season (22 days shorter). Relationships between respiration fluxes and surface soil temperature were similar between years and with those reported in the literature, suggesting that warmer soil temperatures in the oxic surface horizon can largely explain the differences in annual cold season carbon dioxide budgets between the two

450 years. Methane flux and surface soil temperature, by contrast, showed almost reversed relationships between the two years, suggesting that surface soil temperature was not always sufficient to explain methane emission dynamics over the course of this study.

Whilst cold season soil temperatures and FDDs were similar across both years (relative to the 28-year record), we observed that deeper snow pack in Year 1 led to significantly warmer soil temperatures, particularly in the deeper portion of the active

455 soil profile. A regression tree analysis shows that high Year 2 frozen season methane fluxes were clustered from other data along the deep (100 cm) temperature axis at a threshold of -2.4 °C, suggesting inhibited methanogenesis in deeper, anoxic soil horizons. The highest cold season fluxes (among the highest of the two-year study) were observed during Year 1, when deep soil temperatures remained above this threshold whilst surface temperatures were simultaneously below -0.6 °C, suggesting
limited methanotrophy in upper soils being unable to offset methane production at depth. From our data we cannot reliably

460 state that these thresholds represent mechanistic limits, only that they highlight a pattern of temperature dynamics between the upper, oxic layer and the deeper, anoxic layer that are key to controlling surface methane fluxes via their limiting influence on the competing processes of methanotrophy and methanogenesis. These temperature dynamic patterns further explain methane flux dynamics outside of the frozen season during both years. Our results suggest that high cold season methane emission may be associated with warmer atmospheric temperatures and deeper snowpacks, and highlight a need for measurement and mod-

465 elling of soil temperatures throughout all seasons, and throughout the entire active soil profile. Such expansion in observation capacities will allow more accurate prediction of potential changes in the annual methane exchange budget in Arctic tundra regions.

Data availability. Data of this project, including atmospheric mercury, carbon dioxide and methane concentrations and mercury concentration measurements in vegetation, soils and snow are archived with NSF's Arctic Data Center (https://arcticdata.io/), DOI: 10.18739/A21Z41S5S.

470 *Author contributions.* Dean Howard led the analysis of data and manuscript preparation. Yannick Agnan, Detlev Helmig, Yu Yang and Daniel Obrist designed the field measurement campaign. Yannick Agnan, Detlev Helmig and Daniel Obrist conducted field measurements. All authors contributed to writing of the manuscript.

Competing interests. The authors declare that they have no competing interests, financial or otherwise.

Acknowledgements. This study was funded by a by the U.S. Department of Energy (DE-SC0014275) and the U.S. National Science Foun-
475 dation Office of Polar Programs (# OPR 1304305 and 1739567). The authors would like to acknowledge the help of Toolik Field Station for measurement support and the Toolik Field Station Environmental Data Center for providing soil temperature data. We also thank Donald A. (Skip) Walker for allowing the use of the Toolik field maps reproduced in the supplemental material.

References

Agnan, Y., Douglas, T. A., Helmig, D., Hueber, J., and Obrist, D.: Mercury in the Arctic tundra snowpack: temporal and spatial concentration
480   patterns and trace gas exchanges, The Cryosphere, 12, 1939–1956, https://doi.org/10.5194/tc-12-1939-2018, 2018.

Björkman, M. P., Morgner, E., Cooper, E. J., Elberling, B., Klemedtsson, L., and Björk, R. G.: Winter carbon dioxide ef-
fluxes from Arctic ecosystems: An overview and comparison of methodologies, Global Biogeochemical Cycles, 24, 10,
https://doi.org/10.1029/2009GB003667, 2010.

Boone, D. R.: Biological Formation and Consumption of Methane, in: Atmospheric Methane, edited by Khalil, M. A. K., pp. 42–62, Springer,
485   Berlin, Heidelberg, https://doi.org/10.1007/978-3-662-04145-1_4, 2000.

Businger, J. A., Wyngaard, J. C., Izumi, Y., and Bradley, E. F.: Flux-Profile Relationships in the Atmospheric Surface Layer, Journal of
Atmospheric Sciences, 28, 181–189, https://doi.org/10.1175/1520-0469(1971)028<0181:FPRITA>2.0.CO;2, 1971.

Chowdhury, T. R., Herndon, E. M., Phelps, T. J., Elias, D. A., Gu, B., Liang, L., Wullschleger, S. D., and Graham, D. E.: Stoichiometry
and temperature sensitivity of methanogenesis and CO2 production from saturated polygonal tundra in Barrow, Alaska, Global Change
490   Biology, 21, 722–737, https://doi.org/10.1111/gcb.12762, 2015.

Commane, R., Lindaas, J., Benmergui, J., Luus, K. A., Chang, R. Y.-W., Daube, B. C., Euskirchen, E. S., Henderson, J. M., Karion, A.,
Miller, J. B., Miller, S. M., Parazoo, N. C., Randerson, J. T., Sweeney, C., Tans, P., Thoning, K., Veraverbeke, S., Miller, C. E., and Wofsy,
S. C.: Carbon dioxide sources from Alaska driven by increasing early winter respiration from Arctic tundra, Proceedings of the National
Academy of Sciences of the United States of America, 114, 5361–5366, https://doi.org/10.1073/pnas.1618567114, 2017.

495 Conrad, R.: Contribution of hydrogen to methane production and control of hydrogen concentrations in methanogenic soils and sediments,
FEMS Microbiology Ecology, 28, 193–202, https://doi.org/10.1111/j.1574-6941.1999.tb00575.x, 1999.

Dedysh, S. N., Khmelenina, V. N., Suzina, N. E., Trotsenko, Y. A., Semrau, J. D., Liesack, W., and Tiedje, J. M.: Methylocapsa acidiphila
gen. nov., sp. nov., a novel methane-oxidizing and dinitrogen-fixing acidophilic bacterium from Sphagnum bog., International Journal of
Systematic and Evolutionary Microbiology, 52, 251–261, https://doi.org/10.1099/00207713-52-1-251, 2002.

500 Dunfield, P., Knowles, R., Dumont, R., and R.Moore, T.: Methane production and consumption in temperate and subarctic peat soils: Re-
sponse to temperature and pH, Soil Biology and Biochemistry, 25, 321–326, https://doi.org/10.1016/0038-0717(93)90130-4, 1993.

Edwards, G. C., Rasmussen, P. E., Schroeder, W. H., Wallace, D. M., Halfpenny-Mitchell, L., Dias, G. M., Kemp, R. J., and Ausma, S.:
Development and evaluation of a sampling system to determine gaseous Mercury fluxes using an aerodynamic micrometeorological
gradient method, Journal of Geophysical Research: Atmospheres, 110, 11, https://doi.org/10.1029/2004JD005187, 2005.

505 Euskirchen, E. S., Bret-Harte, M. S., Scott, G. J., Edgar, C., and Shaver, G. R.: Seasonal patterns of carbon dioxide and water fluxes in three
representative tundra ecosystems in northern Alaska, Ecosphere, 3, 19, https://doi.org/10.1890/ES11-00202.1, 2012.

Euskirchen, E. S., Bret-Harte, M. S., Shaver, G. R., Edgar, C. W., and Romanovsky, V. E.: Long-Term Release of Carbon Dioxide from
Arctic Tundra Ecosystems in Alaska, Ecosystems, 20, 960–974, https://doi.org/10.1007/s10021-016-0085-9, 2017.

Faïn, X., Helmig, D., Hueber, J., Obrist, D., and Williams, M. W.: Mercury dynamics in the Rocky Mountain, Colorado, snowpack, Biogeo-
510   sciences, 10, 3793–3807, https://doi.org/10.5194/bg-10-3793-2013, 2013.

Foken, T., Göockede, M., Mauder, M., Mahrt, L., Amiro, B., and Munger, W.: Post-Field Data Quality Control, in: Handbook of Microm-
eteorology, edited by Lee, X., Massman, W., and Law, B., pp. 181–208, Springer, Dordrecht, https://doi.org/10.1007/1-4020-2265-4_9,
2004.

Fox, A. M., Huntley, B., Lloyd, C. R., Williams, M., and Baxter, R.: Net ecosystem exchange over heterogeneous Arctic tundra: Scaling
515   between chamber and eddy covariance measurements, Global Biogeochemical Cycles, 22, 15, https://doi.org/10.1029/2007GB003027,
       2008.

Gebauer, R. L. E., Tenhunen, J. D., and Reynolds, J. F.: Soil aeration in relation to soil physical properties, nitrogen availability, and root
       characteristics within an arctic watershed, Plant and Soil, 178, 37–48, https://doi.org/10.1007/BF00011161, 1996.

Gulledge, J., Doyle, A. P., and Schimel, J. P.: Different NH_4^+-inhibition patterns of soil CH_4 consumption: A result of distinct CH_4-oxidizer
520   populations across sites?, Soil Biology and Biochemistry, 29, 13–21, https://doi.org/10.1016/S0038-0717(96)00265-9, 1997.

Hay, L. E. and McCabe, G. J.: Hydrologic effects of climate change in the Yukon River Basin, Climatic Change, 100, 509–523,
       https://doi.org/10.1007/s10584-010-9805-x, 2010.

Hicks Pries, C. E., van Logtestijn, R. S. P., Schuur, E. A. G., Natali, S. M., Cornelissen, J. H. C., Aerts, R., and Dorrepaal, E.: Decadal warming
       causes a consistent and persistent shift from heterotrophic to autotrophic respiration in contrasting permafrost ecosystems, Global Change
525   Biology, 21, 4508–4519, https://doi.org/10.1111/gcb.13032, 2015.

Hugelius, G., Strauss, J., Zubrzycki, S., Harden, J. W., Schuur, E. A. G., Ping, C.-L., Schirrmeister, L., Grosse, G., Michaelson, G. J., Koven,
       C. D., O'Donnell, J. A., Elberling, B., Mishra1, U., Camill1, P., Yu1, Z., Palmtag, J., and Kuhry, P.: Estimated stocks of circumpolar
       permafrost carbon with quantified uncertainty ranges and identified data gaps, Biogeosciences, 11, 6573–6593, https://doi.org/10.5194/bg-
       11-6573-2014, 2014.

530 Joabsson, A., Røjle Christensen, T., and Wallén, B.: Vascular plant controls on methane emissions from northern peatforming wetlands,
       Trends in Ecology & Evolution, 14, 385–388, https://doi.org/10.1016/S0169-5347(99)01649-3, 1999.

Jørgensen, C. J., Johansen, K. M. L., Westergaard-Nielsenand, A., and Elberling, B.: Net regional methane sink in High Arctic soils of
       northeast Greenland, Nature Geoscience, 8, 20–23, https://doi.org/10.1038/NGEO2305, 2015.

Kamal, S. and Varma, A.: Peatland Microbiology, in: Microbiology of Extreme Soils, edited by Dion, P. and Nautiyal, C. S., pp. 177–203,
535   Springer, Berlin, Heidelberg, https://doi.org/10.1007/978-3-540-74231-9_9, 2008.

King, J. Y., Reeburgh, W. S., and Regli, S. K.: Methane emission and transport by arctic sedges in Alaska: Results of a vegetation removal
       experiment, Journal of Geophysical Research: Atmospheres, 103, 29,083–29,092, https://doi.org/10.1029/98JD00052, 1998.

Kljun, N., Calanca, P., Rotach, M. W., and Schmid, H. P.: A simple two-dimensional parameterisation for Flux Footprint Prediction (FFP),
       Geoscientific Model Development, 8, 3695–3713, https://doi.org/10.5194/gmd-8-3695-2015, 2015.

540 Koven, C. D., Riley, W. J., and Stern, A.: Analysis of Permafrost Thermal Dynamics and Response to Climate Change in the CMIP5 Earth
       System Models, Journal of Climate, 26, 1877–1900, https://doi.org/10.1175/JCLI-D-12-00228.1, 2013.

Lai, D. Y. F.: Methane Dynamics in Northern Peatlands: A Review, Pedosphere, 19, 409–421, https://doi.org/10.1016/S1002-0160(09)00003-
       4, 2009.

Le Mer, J. and Roger, P.: Production, oxidation, emission and consumption of methane by soils: A review, European Journal of Soil Biology,
545   37, 25–50, https://doi.org/10.1016/S1164-5563(01)01067-6, 2001.

Lüers, J., Westermann, S., Piel, K., and Boike, J.: Annual CO_2 budget and seasonal CO_2 exchange signals at a high Arctic permafrost site on
       Spitsbergen, Svalbard archipelago, Biogeosciences, 11, 6307–6322, https://doi.org/10.5194/bg-11-6307-2014, 2014.

Maksimova, L. N., Chizhov, A. B., Melamed, V. G., Medvedev, A. V., A.Dubrovin, V., and Dunaeva, E. N.: Estimation of the snow cover
       influence ontemperature regime and seasonal freezing of grounds (with usage of computer) (in Russian), in: Frozen Rocks and Snow
550   Cover, edited by Voitkovskii, K. F., pp. 127–135, Nauka, Moscow, 1977.

Mastepanov, M., Sigsgaard, C., Tagesson, T., Ström1, L., Tamstorf, M. P., Lund, M., and Christensen, T. R.: Revisiting factors controlling methane emissions from high-Arctic tundra, Biogeosciences, 10, 5139–5158, https://doi.org/10.5194/bg-10-5139-2013, 2013.

Natali, S. M., Schuur, E. A. G., Mauritz, M., Schade, J. D., Celis, G., Crummer, K. G., Johnston, C., Krapek, J., Pegoraro, E., Salmon, V. G., and Webb, E. E.: Permafrost thaw and soil moisture driving CO_2 and CH_4 release from upland tundra, Journal of Geophysical Research: Biogeosciences, 120, 525–537, https://doi.org/10.1002/2014JG002872, 2015.

Obrist, D., Agnan, Y., Jiskra, M., Olson, C. L., Colegrove, D. P., Hueber, J., Moore, C. W., Sonke, J. E., and Helmig, D.: Tundra uptake of atmospheric elemental mercury drives Arctic mercury pollution, Nature, 547, 201–204, https://doi.org/10.1038/nature22997, 2017.

Oechel, W. C., Vourlitis, G. L., Verfaillie JR., J., Crawford, T., Brooks, S., Dumas, E., Hope, A., Stow, D., Boynton, B., Nosov, V., and Zulueta, R.: A scaling approach for quantifying the net CO_2 flux of the Kuparuk River Basin, Alaska, Global Change Biology, 6, 160–173, https://doi.org/10.1046/j.1365-2486.2000.06018.x, 2008.

Oechel, W. C., Laskowski, C. A., Burba, G., Gioli, B., and Kalhori, A. A. M.: Annual patterns and budget of CO_2 flux in an Arctic tussock tundra ecosystem, Journal of Geophysical Research: Biogeosciences, 119, 323–339, https://doi.org/10.1002/2013JG002431, 2014.

Olson, C., Jiskra, M., Biester, H., Chow, J., and Obrist, D.: Mercury in Active-Layer Tundra Soils of Alaska: Concentrations, Pools, Origins, and Spatial Distribution, Global Biogeochemical Cycles, 32, 1058–1073, https://doi.org/10.1029/2017GB005840, 2018.

Panikov, N. S. and Dedysh, S. N.: Cold season CH_4 and CO_2 emission from boreal peat bogs (West Siberia): Winter fluxes and thaw activation dynamics, Global Biogeochemical Cycles, 14, 1071–1080, https://doi.org/10.1029/1999GB900097, 2000.

Polyakov, I. V., Alekseev, G. V., Bekryaev, R. V., Bhatt, U., Colony, R. L., Johnson, M. A., Karklin, V. P., Makshtas, A. P., Walsh, D., and Yulin, A. V.: Observationally based assessment of polar amplification of global warming, Geophysical Research Letters, 29, 4, https://doi.org/10.1029/2001GL011111, 2002.

Preuss, I., Knoblauch, C., Gebert, J., , and Pfeiffer, E.-M.: Improved quantification of microbial CH_4 oxidation efficiency in arctic wetland soils using carbon isotope fractionation, Biogeosciences, 10, 2539–2552, https://doi.org/10.5194/bg-10-2539-2013, 2013.

Richter, L.: Temperature Dependence of Net Methane Oxidation in Arctic Soils Under Aerobic Conditions, Master's thesis, University of Massachusetts Lowell, Lowell, Massachusetts, USA, 2019.

Riley, W. J., Subin, Z. M., Lawrence, D. M., Swenson, S. C., Torn, M. S., Meng, L., Mahowald, N. M., and Hess, P.: Barriers to predicting changes in global terrestrial methane fluxes: analyses using CLM4Me, a methane biogeochemistry model integrated in CESM, Biogeosciences, 8, 1925–1953, https://doi.org/10.5194/bg-8-1925-2011, 2011.

Rivkina, E., Laurinavichius, K., McGrath, J., Tiedje, J., Shcherbakova, V., and Gilichinsky, D.: Microbial life in permafrost, Advances in Space Research, 33, 1215–1221, https://doi.org/10.1016/j.asr.2003.06.024, 2004.

Romanovsky, V. E., Smith, S. L., and Christiansen, H. H.: Permafrost thermal state in the polar Northern Hemisphere during the international polar year 2007–2009: a synthesis, Permafrost and Periglacial Processes, 21, 106–116, https://doi.org/10.1002/ppp.689, 2010.

Sachs, T., Wille, C., Boike, J., and Kutzbach, L.: Environmental controls on ecosystem-scale CH_4 emission from polygonal tundra in the Lena River Delta, Siberia, Journal of Geophysical Research: Biogeosciences, 113, 12, https://doi.org/10.1029/2007JG000505, 2008.

Schimel, J. P.: Plant transport and methane production as controls on methane flux from arctic wet meadow tundra, Biogeochemistry, 28, 183–200, https://doi.org/10.1007/BF02186458, 1995.

Schuur, E. A. G., Vogel, J. G., Crummer, K. G., Lee, H., Sickman, J. O., and Osterkamp, T. E.: The effect of permafrost thaw on old carbon release and net carbon exchange from tundra, Nature, 459, 556–553, https://doi.org/10.1038/nature08031, 2009.

Schuur, E. A. G., McGuire, A. D., Schädel, C., Grosse, G., Harden, J. W., Hayes, D. J., Hugelius, G., Koven, C. D., Kuhry, P., Lawrence, D. M., Natali, S. M., Olefeldt, D., Romanovsky, V. E., Schaefer, K., Turetsky, M. R., Treat, C. C., and Vonk, J. E.: Climate change and the permafrost carbon feedback, Nature, 520, 171–179, https://doi.org/10.1038/nature14338, 2015.

590 Seok, B., Helmig, D., Williams, M. W., Liptzin, D., Chowanski, K., and Hueber, J.: An automated system for continuous measurements of trace gas fluxes through snow: an evaluation of the gas diffusion method at a subalpine forest site, Niwot Ridge, Colorado, Biogeochemistry, 95, 95–113, https://doi.org/10.1007/s10533-009-9302-3, 2009.

Shaver, G. R. and Chapin III, F. S.: Production: Biomass Relationships and Element Cycling in Contrasting Arctic Vegetation Types, Ecological Monographs, 61, 1–31, https://doi.org/10.2307/1942997, 1991.

595 Sokratov, S. A. and Barry, R. G.: Intraseasonal variation in the thermoinsulation effect of snow cover on soil temperatures and energy balance, Journal of Geophysical Research: Atmospheres, 107, 6, https://doi.org/10.1029/2001JD000489, 2002.

Sweeney, C., Dlugokencky, E., Miller, C. E., Wofsy, S., Karion, A., Dinardo, S., Chang, R. Y.-W., Miller, J. B., Bruhwiler, L., Crotwell, A. M., Newberger, T., McKain, K., Stone, R. S., Wolter, S. E., Lang, P. E., and Tans, P.: No significant increase in long-term CH_4 emissions on North Slope of Alaska despite significant increase in air temperature, Geophysical Research Letters, 43, 6604–6611, 600 https://doi.org/10.1002/2016GL069292, 2016.

Verville, J. H., Hobbie, S. E., Chapin III, F. S., and Hooper, D. U.: Response of tundra CH_4 and CO_2 flux to manipulation of temperature and vegetation, Biogeochemistry, 41, 215–235, https://doi.org/10.1023/A:1005984701775, 1998.

Vonk, J. E. and Gustafsson, Ö.: Permafrost-carbon complexities, Nature Geoscience, 6, 675–676, https://doi.org/10.1038/ngeo1937, 2013.

Whalen, S. C.: Biogeochemistry of Methane Exchange between Natural Wetlands and the Atmosphere, Environmental Engineering Science, 605 22, https://doi.org/10.1089/ees.2005.22.73, 2005.

Woodruff, B. L.: Sampling Error in a Single-instument Vertical Gradient Measurement in the Atmospheric Surface Layer, Master's thesis, Colorado State University, Fort Collins, Colorado, USA, 1986.

Wutzler, T., Lucas-Moffat, A., Migliavacca, M., Knauer, J., Sickel, K., Šigut, L., Menzer, O., and Reichstein, M.: Basic and extensible post-processing of eddy covariance flux data with REddyProc, Biogeosciences, 15, 5015–5030, https://doi.org/10.5194/bg-15-5015-2018, 610 2018.

Yvon-Durocher, G., Allen, A. P., Bastviken, D., Conrad, R., Gudasz, C., St-Pierre, A., Thanh-Duc, N., and del Giorgio, P. A.: Methane fluxes show consistent temperature dependence across microbial to ecosystem scales, Nature, 507, 488–491, https://doi.org/10.1038/nature13164, 2014.

Zhu, X., Zhuang, Q., Lu, X., and Song, L.: Spatial scale-dependent land–atmospheric methane exchanges in the northern high latitudes from 615 1993 to 2004, Biogeosciences, 11, 1693–1704, https://doi.org/10.5194/bg-11-1693-2014, 2014.

Zona, D., Gioli, B., Commane, R., Lindaas, J., Wofsy, S. C., Miller, C. E., Dinardo, S. J., Dengel, S., Sweeney, C., Karion, A., Chang, R. Y.-W., Henderson, J. M., Murphy, P. C., Goodrich, J. P., Moreaux, V., Liljedahl, A., Watts, J. D., Kimball, J. S., Lipson, D. A., and Oechel, W. C.: Cold season emissions dominate the Arctic tundra methane budget, Proceedings of the National Academy of Sciences of the United States of America, 113, 40–45, https://doi.org/10.1073/pnas.1516017113, 2016.
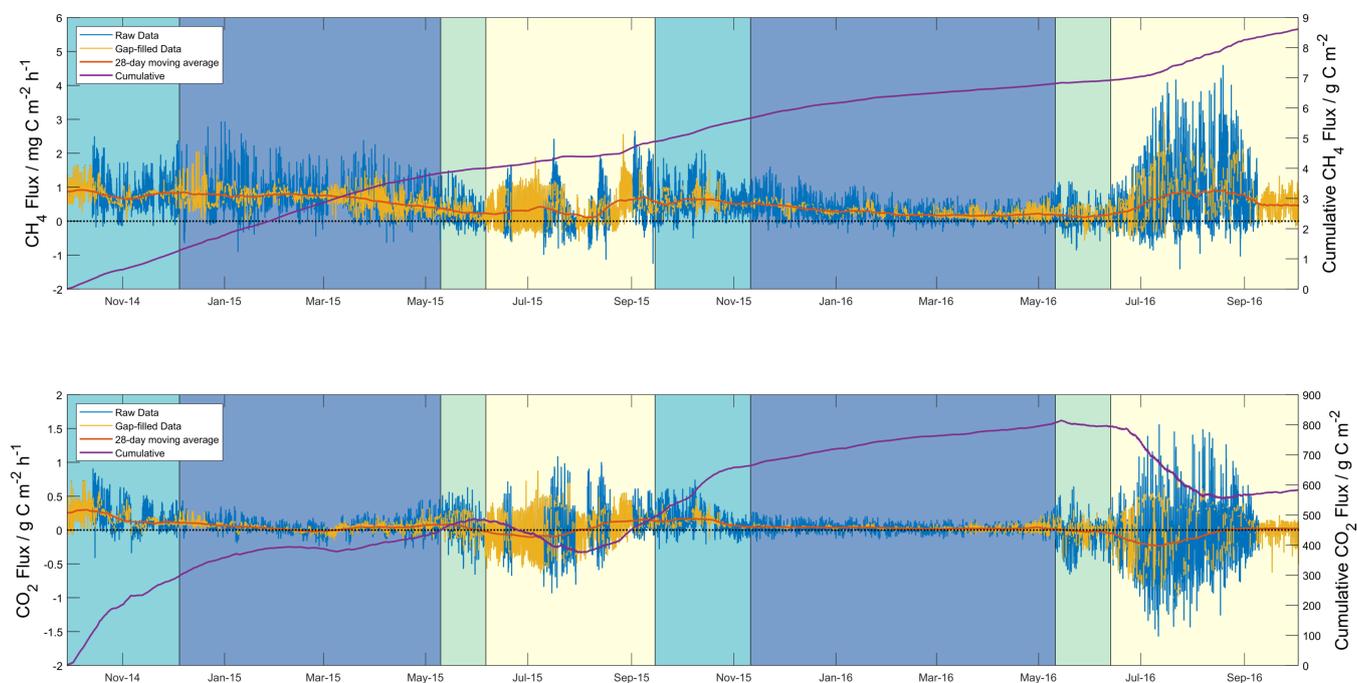
Figure 1. Half-hourly measured (blue lines) and gap-filled (yellow lines), and cumulative flux data (purple lines) for methane (upper panel) and carbon dioxide (lower panel). 28-day centred moving averages (red lines) have been included based on half-hourly flux data. Shading shows seasons (as defined in the text) for both years beginning with freezing (turquoise), then frozen (blue), thawing (green) and active (yellow).
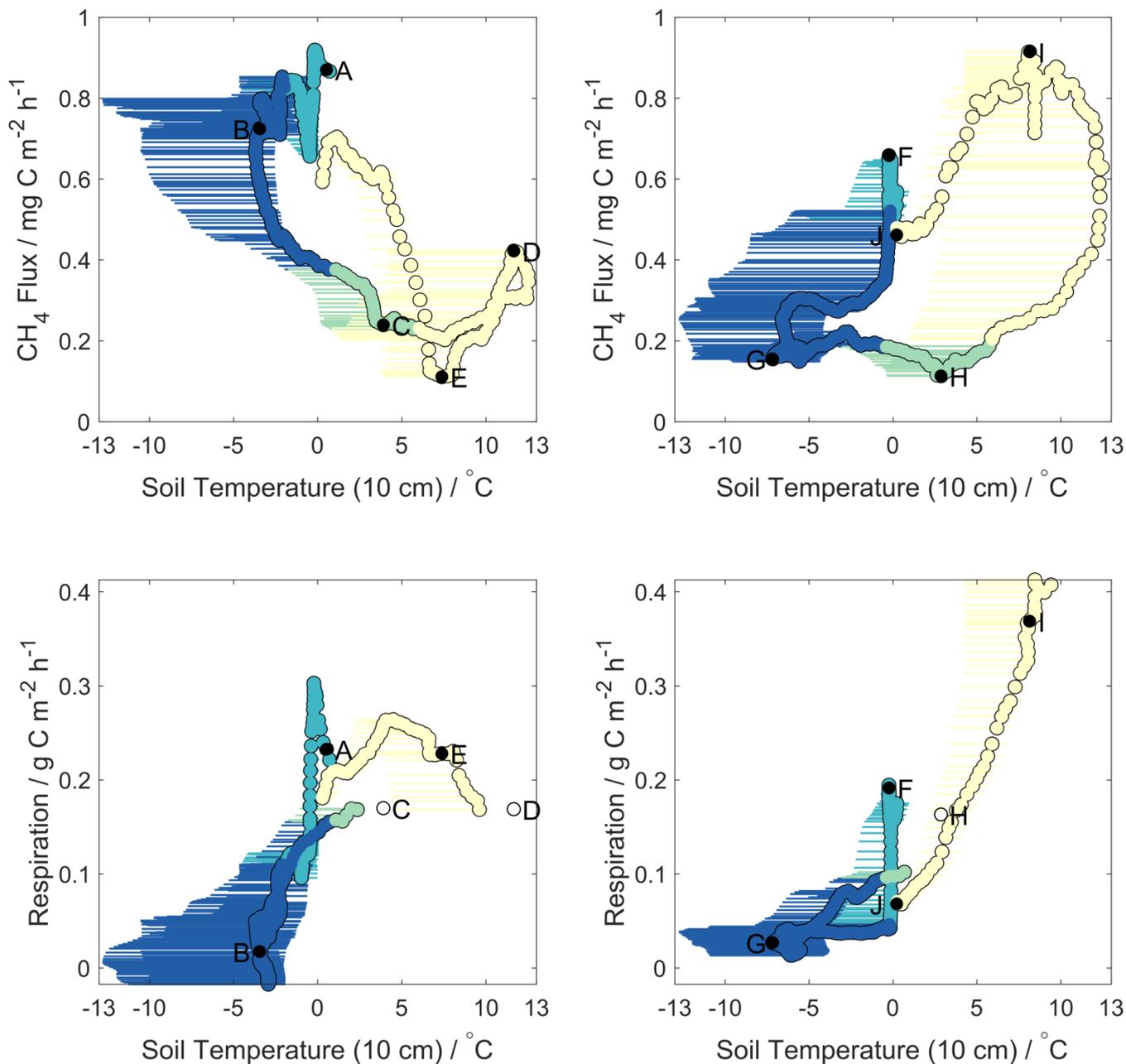
Figure 2. Methane (upper panels) and respiration (lower panels) fluxes against soil temperatures for Year 1 (left panels) and Year 2 (right panels). Horizontal error bars represent the range of soil temperatures across all four sampling pits, circles represent values used in decision tree analysis (average of both Toolik Field Station profiles). Colours correspond to seasons as in Fig. 1. Lettering on methane flux plots are sequential in time and correspond to those shown in Fig. 4. Lettering on respiration plots are given for the same times as those in methane plots. Open circles represent times for which respiration data are missing – respiration values here are linearly interpolated in time between the closest known values.
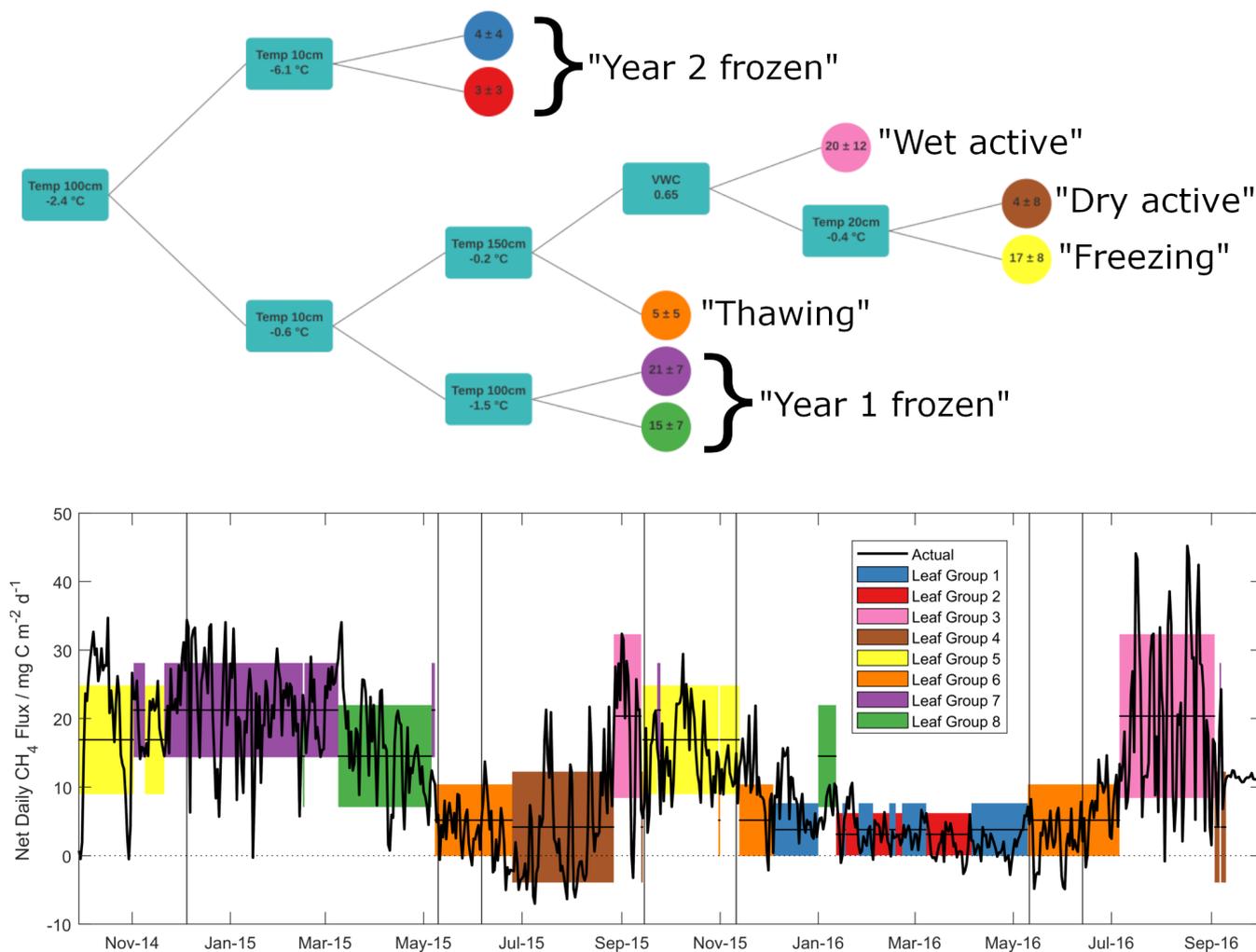
Figure 3. Outcome of the regression tree analysis (upper panel), giving decision steps and outcomes (mean $\pm$ standard deviation in mg C m^{-2} d^{-1}) of selected methane emission data. Turquoise squares give the variable and thresholds around which decisions are made – lines pointing upwards correspond to values above this threshold and lines pointing down to values below. Lower panel shows net daily methane flux data (black line), along with means (horizontal lines) and standard deviations (shaded regions) of input data, as grouped by the regression tree in upper panel. Note that all methane flux data are net daily sums.
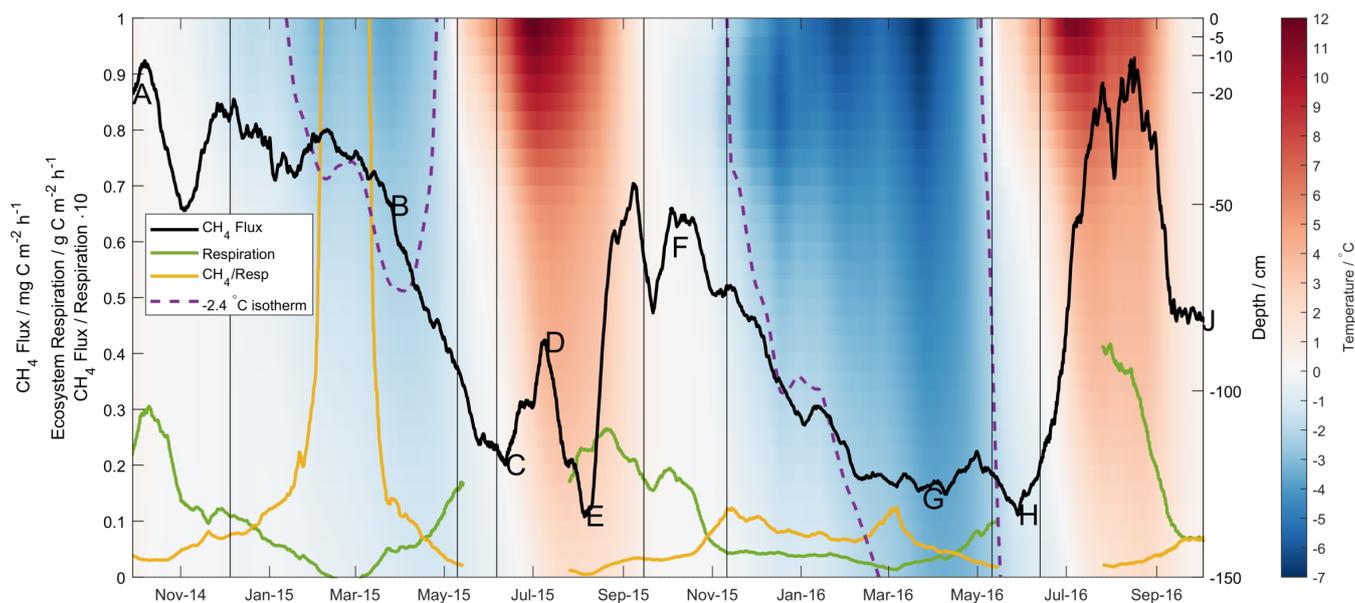
Figure 4. 28-day moving average methane (black line) and ecosystem respiration (green line) fluxes, along with the ratio of the two (yellow line). Lettering corresponds in time to that given in Fig. 2. Shading gives soil temperature as measured at Toolik Field Station according to depth (right axis). Purple dotted line shows the depth of the -2.4 °C isotherm.

Table 1. Overview of methane fluxes split according to season. Values in parentheses in cumulative columns are percentages of the total for that year. Daily differences are the differences in mean daily fluxes for that season between the two years, with p-statistics from Student's two-sample t-test giving the significance with which the null hypothesis (values come from distributions with same mean) can be rejected.

	Year 1 29 Sep 2014 – 14 Sep 2015			Year 2 15 Sep 2015 – 03 Oct 2016			Daily Difference
	Duration days	Cumulative g C m^{-2}	Daily mg C m^{-2} d^{-1}	Duration days	Cumulative g C m^{-2}	Daily mg C m^{-2} d^{-1}	Value (p) mg C m^{-2} d^{-1}
Freezing	66	1.3 (27%)	19 ± 4	56	0.8 (21%)	14 ± 4	5 (<0.001)
Frozen	155	2.5 (51%)	16 ± 5	181	1.1 (30%)	6 ± 3	10 (<0.001)
Thawing	26	0.2 (4%)	6 ± 2	32	0.1 (3%)	3 ± 2	3 (0.003)
Active	100	0.9 (18%)	9 ± 8	111	1.7 (46%)	15 ± 9	6 (<0.001)
Total	347	4.9		380	3.7		

Table 2. As for Table 1, for carbon dioxide fluxes. Seasonal percentages are represented as the absolute value of net seasonal exchange as a proportion of the annual total. As seasonal net totals are bi-directional, these percentages do not necessarily add to 100.

	Year 1 29 Sep 2014 – 14 Sep 2015			Year 2 15 Sep 2015 – 03 Oct 2016			Daily Difference
	Duration days	Cumulative g C m^{-2}	Daily g C m^{-2} d^{-1}	Duration days	Cumulative g C m^{-2}	Daily g C m^{-2} d^{-1}	Value (p) g C m^{-2} d^{-1}
Freezing	66	293 (60%)	4 ± 3	56	167 (188%)	3 ± 2	1.5 (0.001)
Frozen	155	148 (31%)	1 ± 1	181	142 (106%)	0.8 ± 0.5	0.2 (0.04)
Thawing	26	30 (6%)	1 ± 2	32	-15 (17%)	0 ± 1	1.6 (<0.001)
Active	100	14 (3%)	0 ± 3	111	-211 (237%)	-2 ± 3	2.0 (<0.001)
Total	347	485		380	89		